Scientific Research Publishing

American Journal of Computational Mathematics, 2025, 15(3), 259-277
https://www.scirp.org/journal/ajcm
ISSN Online: 2161-1211
ISSN Print: 2161-1203

Numerical Investigation of MHD Heat Transfer in a Nanofluid Trapezoidal Cavity with Embedded Square Heat Sources

Sree Pradip Kumer Sarker*, Mohammad Mahmud Alam

Department of Mathematics, Dhaka University of Engineering and Technology (DUET), Gazipur, Bangladesh
Email: *pradip.duet@gmail.com, alamdr.mahmud@duet.ac.bd

How to cite this paper: Sarker, S.P.K. and Alam, M.M. (2025) Numerical Investigation of MHD Heat Transfer in a Nanofluid Trapezoidal Cavity with Embedded Square Heat Sources. *American Journal of Computational Mathematics*, **15**, 259-277.
https://doi.org/10.4236/ajcm.2025.153014

Received: July 16, 2025
Accepted: August 4, 2025
Published: August 7, 2025

Abstract

This study presents a comprehensive numerical investigation of magnetohydrodynamic (MHD) heat transfer within a trapezoidal cavity filled with a Cu–H_2O nanofluid and containing two symmetrically embedded square heat sources. The effects of varying nanoparticle volume fractions (ϕ = 0.01, 0.02, and 0.03), Hartmann number (Ha = 0, 30), and Rayleigh number (Ra = 10^3 - 10^6) were analyzed to assess flow and thermal behaviors. The governing equations for incompressible, laminar flow and heat transfer were solved using COMSOL Multiphysics under steady-state conditions. Velocity and temperature contours reveal that increasing Ra enhances convective heat transfer, with pronounced thermal gradients and stronger circulation cells. Conversely, higher Ha values suppress fluid motion due to the Lorentz force, reducing convective effects and promoting conduction. At higher nanoparticle concentrations, thermal conductivity improves, intensifying heat transfer despite magnetic damping. The sinusoidal upper wall and trapezoidal cavity shape introduce complex flow interactions, especially near the embedded heat sources. Velocity profiles show peak flow intensities around the heated regions, while temperature fields confirm improved thermal distribution with increasing ϕ. Results highlight the significant role of magnetization and nanoparticle concentration in optimizing heat transfer in nanofluid systems. The findings offer valuable insights for designing thermal systems such as electronic cooling devices and energy storage systems, where enhanced convective performance in confined geometries is essential.

Keywords

Magnetohydrodynamics, Nanofluid, Trapezoidal Cavity, Natural Convection, Thermal Conductivity

1. Introduction

The study of heat transfer enhancement in enclosures using nanofluids under magnetohydrodynamic (MHD) influences has gained substantial momentum due to its applicability in advanced thermal systems such as electronic cooling, solar collectors, and energy storage devices [1]-[4]. Trapezoidal and other non-standard geometries have emerged as preferred domains for analyzing natural and mixed convection processes, particularly when integrated with internal heat sources or structural complexities like sinusoidal walls [5]-[8]. Nanofluids, especially Cu-H_2O and hybrid formulations, have shown significant improvements in thermal performance due to their enhanced thermophysical properties [9]-[12]. When coupled with external magnetic fields, these nanofluids facilitate control over boundary layer dynamics and flow stability, making them ideal for MHD studies in corrugated, porous, and wavy enclosures [13]-[16]. The impact of wall undulation, inclination, and boundary modulation has been explored extensively, confirming their ability to intensify thermal gradients and promote convective mixing [17]-[20].

The presence of internal features, such as solid cylinders, triangular or square blocks, and especially geometrically complex star-shaped heat sources, introduces additional degrees of thermal control and entropy management [21]-[24]. These embedded elements influence local flow recirculation, vortex generation, and entropy generation patterns, all critical for performance optimization [25]-[28]. Numerical studies employing finite element and finite volume approaches have validated their capacity to model intricate heat-fluid interactions under varied thermal and magnetic conditions [29]-[33]. Recent work has focused on enhancing thermal control through Multiphysics strategies involving thermal radiation, oscillating magnetic fields, and variable fluid properties [34]-[36]. Moreover, the use of optimization tools such as response surface methodology and parametric sensitivity analysis has led to systematic performance improvement across diverse configurations [37]-[42]. Investigations into ferrofluid behavior, rotating elements, and non-Newtonian effects in trapezoidal and wavy cavities continue to expand the scope of MHD-nanofluid research [43]-[45].

In this context, the current study numerically examines MHD-driven natural convection in an inclined trapezoidal cavity filled with Cu–H_2O nanofluid, featuring a sinusoidal upper wall and embedded square heat-generating elements. By analyzing the influence of Rayleigh number, Hartmann number, and nanoparticle volume fraction, this research aims to provide design insights for optimizing heat transfer in complex engineering applications.

2. Model Description

The computational domain consists of a two-dimensional inclined trapezoidal cavity filled with a Cu–H_2O nanofluid, as illustrated in **Figure 1**. Two identical square copper heat sources are embedded symmetrically in the nanofluid region, positioned horizontally at mid-height ($H/2$) and separated by a distance of $L/2$.

The top surface of the cavity is sinusoidally wavy, and the sidewalls are inclined at an angle γ. A uniform transverse magnetic field B_0 is applied in the negative x-direction, influencing the flow field through Lorentz force effects.

The natural convection is driven by internal heat generation within the copper blocks and thermal gradients imposed by the boundary conditions. The flow is assumed to be steady, laminar, two-dimensional, and governed by the Boussinesq approximation. All fluid and thermal properties of the nanofluid are temperature-independent except for the density variation contributing to buoyancy.

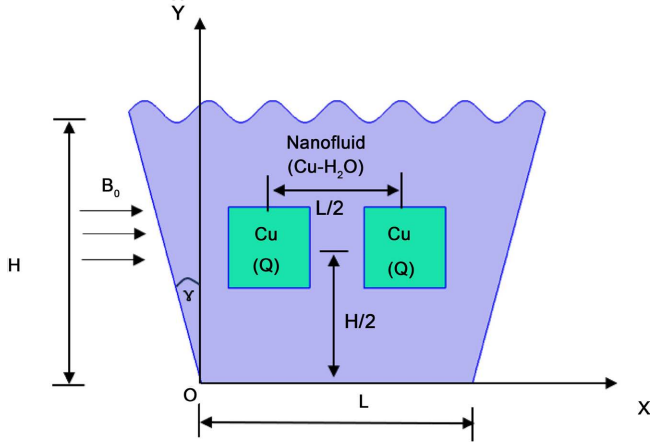

Figure 1. Geometry.

The thermal boundary conditions applied to the cavity walls and internal obstacles are summarized in Table 1.

Table 1. Boundary condition.

Boundary	Condition	Temperature Value
Top Wavy Wall	Isothermal	$T = T_m$
Bottom Wall	Isothermal	$T = T_m$
Left & Right Walls	Thermal Insulation (Adiabatic)	$n \cdot \nabla T = 0$
Square Obstacles	Internal Heat Source	Volumetric heating Q

All solid walls are subjected to the no-slip velocity condition $\vec{u} = 0$. The simulations are performed using the finite element method in COMSOL Multiphysics, focusing on the interplay between Rayleigh number, Hartmann number, and nanoparticle volume fraction.

3. Mathematical Modeling

This study addresses the conjugate magnetohydrodynamic (MHD) free convection within an inclined trapezoidal cavity saturated with a Cu–H_2O nanofluid. The enclosure contains two symmetrically embedded square copper heat sources that generate internal volumetric heating. A uniform magnetic field is applied perpen-

dicular to the inclined sidewall, inducing a Lorentz force that influences the nanofluid flow dynamics.

The working fluid is modeled as a single-phase nanofluid with thermophysical properties dependent on the nanoparticle volume fraction. The flow is assumed to be laminar, steady-state, two-dimensional, and incompressible. The Boussinesq approximation is applied to account for buoyancy effects due to temperature variation.

Governing Equations:

The physical model is governed by the following conservation equations:

$$\frac{\partial u}{\partial x}+\frac{\partial v}{\partial y}=0 \tag{1}$$

$$\rho_{nf}\left(u\frac{\partial u}{\partial x}+v\frac{\partial u}{\partial y}\right)=-\frac{\partial p}{\partial x}+\mu_{nf}\left(\frac{\partial^2 u}{\partial x^2}+\frac{\partial^2 u}{\partial y^2}\right)+\rho_{nf}g\beta_{nf}\left(T-T_c\right)\sin\left(\gamma\right)-\sigma_{nf}\beta_0^2 u \tag{2}$$

$$\rho_{nf}\left(u\frac{\partial v}{\partial x}+v\frac{\partial v}{\partial y}\right)=-\frac{\partial p}{\partial y}+\mu_{nf}\left(\frac{\partial^2 v}{\partial x^2}+\frac{\partial^2 v}{\partial y^2}\right)+\rho_{nf}g\beta_{nf}\left(T-T_c\right)\cos\left(\gamma\right)-\sigma_{nf}\beta_0^2 v \tag{3}$$

$$\rho_{nf}c_{p,nf}\left(u\frac{\partial T}{\partial x}+v\frac{\partial T}{\partial y}\right)=k_{nf}\left(\frac{\partial^2 T}{\partial x^2}+\frac{\partial^2 T}{\partial y^2}\right)+Q \tag{4}$$

Nanofluid Property:

$$\rho_{nf}=\left(1-\phi\right)\rho_f+\phi\rho_s \tag{5}$$

$$\left(\rho c_p\right)_{nf}=\left(1-\phi\right)\left(\rho c_p\right)_f+\phi\left(\rho c_p\right)_s \tag{6}$$

$$\mu_{nf}=\frac{\mu_f}{\left(1-\phi\right)^{2.5}} \tag{7}$$

$$k_{nf}=k_f\left[\frac{k_s+2k_f-2\phi\left(k_f-k_s\right)}{k_s+2k_f+\phi\left(k_f-k_s\right)}\right] \tag{8}$$

$$\beta_{nf}=\frac{\left(1-\phi\right)\rho_f\beta_f+\phi\rho_s\beta_s}{\rho_{nf}} \tag{9}$$

Non-Dimensional Equations:

$$X=\frac{x}{L},Y=\frac{y}{L},U=\frac{uL}{\alpha_f},V=\frac{vL}{\alpha_f},\theta=\frac{T-T_c}{T_h-T_c},P=\frac{pL^2}{\mu_{nf}},\text{here},\alpha_f=\frac{k_f}{\rho_f c_{p,f}} \tag{10}$$

$$Ra=\frac{g\beta_{nf}\left(T_h-T_c\right)L^3}{\nu_{nf}\alpha_f},Pr=\frac{\nu_f}{\alpha_f},Ha=\beta_0 L\sqrt{\frac{\sigma_{nf}}{\mu_{nf}}},Q^*=\frac{QL^2}{k_{nf}\left(T_h-T_c\right)} \tag{11}$$

$$\frac{\partial U}{\partial X}+\frac{\partial V}{\partial Y}=0 \tag{12}$$

$$U\frac{\partial U}{\partial X}+V\frac{\partial U}{\partial Y}=-\frac{\partial P}{\partial X}+\frac{\mu_{nf}}{\mu_f}\left(\frac{\partial^2 U}{\partial X^2}+\frac{\partial^2 U}{\partial Y^2}\right)+RaPr\frac{\rho_{nf}\beta_{nf}}{\rho_f\beta_f}\theta\sin\left(\gamma\right)-Ha^2U \tag{13}$$

$$U\frac{\partial V}{\partial X}+V\frac{\partial V}{\partial Y}=-\frac{\partial P}{\partial X}+\frac{\mu_{nf}}{\mu_f}\left(\frac{\partial^2 V}{\partial X^2}+\frac{\partial^2 V}{\partial Y^2}\right)+RaPr\frac{\rho_{nf}\beta_{nf}}{\rho_f\beta_f}\theta\cos\left(\gamma\right)-Ha^2U \tag{14}$$

$$U\frac{\partial\theta}{\partial X}+V\frac{\partial\theta}{\partial Y}=\frac{k_{nf}}{k_f}\frac{1}{Pr}\left(\frac{\partial^2\theta}{\partial X^2}+\frac{\partial^2\theta}{\partial Y^2}\right)+Q^* \tag{15}$$

Here, Q^* represents the volumetric internal heat generation in the square heat sources, and T_m is the reference temperature.

Nanofluid Property:

$$\frac{\rho_{nf}}{\rho_f}=(1-\phi)+\phi\frac{\rho_s}{\rho_f} \tag{16}$$

$$\frac{(\rho c_p)_{nf}}{(\rho c_p)_f}=(1-\phi)+\phi\frac{(\rho c_p)_s}{(\rho c_p)_f} \tag{17}$$

$$\frac{\mu_{nf}}{\mu_f}=\frac{1}{(1-\phi)^{2.5}} \tag{18}$$

$$\frac{k_{nf}}{k_f}=\frac{k_s+2k_f-2\phi(k_f-k_s)}{k_s+2k_f+\phi(k_f-k_s)} \tag{19}$$

$$\beta_{nf}\rho_{nf}=(1-\phi)\rho_f\beta_f+\phi\rho_s\beta_s \tag{20}$$

The convective heat transfer is quantified using the local and average Nusselt numbers at the top wavy surface:

$$Nu_{Local}=-\left.\frac{\partial\theta}{\partial n}\right|_{\text{Wavy-Wall}} \tag{21}$$

$$\bar{N}u=\frac{1}{L_w}\int_0^{L_w}Nu_{Local}\mathrm{d}X=-\frac{1}{L_w}\int_0^{L_w}\frac{\partial\theta}{\partial n}\mathrm{d}X \tag{22}$$

Here, L_w is the arc length of the top wavy wall.

Dimensional Local Entropy Generation Rate:

$$S_t=\frac{k_{hnf}}{T_{ref}^2}+\left[\left(\frac{\partial T}{\partial x}\right)^2+\left(\frac{\partial T}{\partial y}\right)^2\right]+\frac{\mu_{hnf}}{T_{ref}}\left[2\left(\frac{\partial u}{\partial x}\right)^2+2\left(\frac{\partial v}{\partial y}\right)^2+\left(\frac{\partial v}{\partial x}+\frac{\partial u}{\partial y}\right)^2\right]+\sigma_{hnf}\beta_0^2v^2 \tag{23}$$

where, k_{hnf}, μ_{hnf} and σ_{hnf} are Thermal Conductivity, Dynamic Viscosity, and Electrical Conductivity of the nanofluid. $T_{ref}=(T_h+T_c)/2$ is the reference temperature, B_0 is the magnetic field intensity in the vertical direction. u and v are the velocity components in x and y directions.

Non-Dimensional Entropy Generation Rate:

$$\begin{aligned}S_t=&\left(\frac{T_{ref}H}{k_f(T_h-T_c)}\right)^2\left[k_{hnf}\left(\left(\frac{\partial\theta}{\partial X}\right)^2+\left(\frac{\partial\theta}{\partial Y}\right)^2\right)\right.\\&\left.+\mu_{hnf}\chi\left(2\left(\frac{\partial U}{\partial X}\right)^2+2\left(\frac{\partial V}{\partial X}\right)^2+\left(\frac{\partial V}{\partial X}+\frac{\partial U}{\partial Y}\right)^2\right)\right]+\sigma_{hnf}Ha^2V\end{aligned} \tag{24}$$

where, $\chi=\frac{\mu_f\alpha_f^2T_{ref}}{k_fH^2(T_h-T_c)^2}, T_{ref}=\frac{T_h+T_c}{2}$

Total Entropy Generation (Volume-Averaged):

$$S_t = \frac{1}{V}\int_V S_t \mathrm{d}V \tag{25}$$

Thermal Performance Criterion (TPC):

$$TPC = \frac{S_t}{N_u} \tag{26}$$

Thermophysical Parameters

The thermophysical properties of copper nanoparticles and pure water are summarized in Table 2, while the nanofluid properties for varying volume fractions are detailed in Table 3. As shown in Table 2, copper possesses significantly higher thermal and electrical conductivity compared to water, which enhances heat transfer performance. In contrast, water exhibits a higher specific heat capacity and thermal expansion coefficient, favoring buoyancy-driven convection.

Table 2. Thermophysical properties of pure water and Copper nanoparticles.

Thermophysical Properties	Copper Nanoparticles	Pure Water
ρ (kg/m^3)	8933	996.60
C_p (J/kg·K)	385	4179.20
k (W/m·K)	401	0.6102
β (1/K)	4.99×10^{-5}	2.66×10^{-4}
σ (1/Ω·m)	5.96×10^{-7}	5.50×10^{-6}

Table 3. Properties of nanofluid.

Property	Unit	Volume Fraction of Nanoparticles		
		0.01	0.02	0.03
Density (ρ)	kg/m^3	1076.00	1155.30	1234.70
Specific heat (C_p)	J/kg·K	3864.20	3592.50	3355.70
Thermal conductivity (k)	W/m·K	0.62861	0.64739	0.66655
Dynamic viscosity (μ)	kg/m·s	8.7552×10^{-4}	8.9803×10^{-4}	9.2135×10^{-4}
Electric conductivity (σ)	$\Omega^{-1}\cdot m^{-1}$	5.6667×10^{-6}	5.8367×10^{-6}	6.0103×10^{-6}
Thermal diffusivity (α)	m^2/s	1.4651×10^{-7}	1.4651×10^{-7}	1.465×10^{-7}
Volumetric expansion (β)	K^{-1}	2.4806×10^{-4}	2.3258×10^{-4}	2.191×10^{-4}

Table 3 outlines the effective thermophysical properties of the Cu–H_2O nanofluid for volume fractions ϕ = 0.01, 0.02, and 0.03. With increasing ϕ, the nanofluid's density, thermal conductivity, dynamic viscosity, and electrical conductivity increase, while the specific heat and thermal expansion decrease. This highlights a balance between improved thermal conductivity and the rise in viscous resistance, which directly influences the overall flow and thermal behavior within the cavity.

4. Results and Discussion

4.1. Verification

To ensure the accuracy and reliability of the present numerical model, a validation study was conducted by comparing the streamline contours with those reported in Ref. [45]. As illustrated in **Figure 2**, both the reference and current simulations depict a similar vortex structure, flow pattern, and circulation intensity around the central heat-generating circular obstacle. The core recirculation zones and streamline curvature show excellent consistency, indicating that the present computational approach and boundary condition implementation are robust and in agreement with established literature.

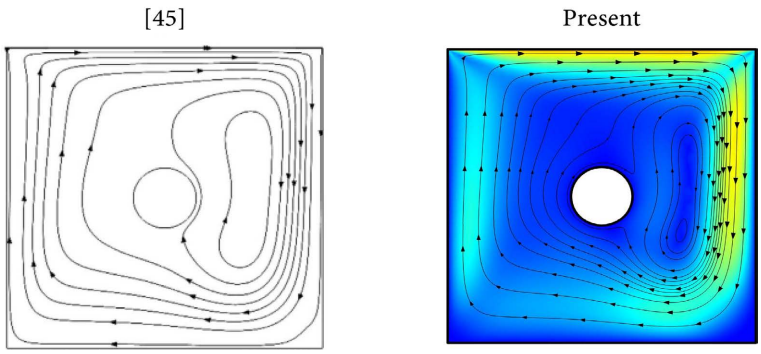

Figure 2. Comparison of the Streamline in the present study and the Ref. [45].

This agreement validates the finite element-based formulation and boundary setup used in COMSOL Multiphysics for modeling MHD-driven natural convection in complex geometries with internal heat generation. As such, the model is considered reliable for further parametric analysis involving variations in Rayleigh number, Hartmann number, and nanoparticle volume fraction.

4.2. Discussion

The effects of Rayleigh number (Ra), Hartmann number (Ha), and nanoparticle volume fraction (ϕ) on velocity and temperature distribution are presented in **Figures 3-8**. These results elucidate the fluid flow structure and thermal transport mechanisms under varying physical conditions within the trapezoidal nanofluid-filled cavity.

Figure 3: **Velocity Contours for $\phi = 0.01$:**

At $Ra = 10^3$ and $Ha = 0$, weak natural convection results in small, symmetric recirculation zones adjacent to the heated blocks. As Ra increases to 10^6, the buoyancy force strengthens, enhancing vortex formation and generating a primary circulation cell that dominates the cavity. When $Ha = 30$ is applied, the flow field is significantly dampened at all Ra levels, especially at higher Ra where the Lorentz force suppresses the circulation intensity, reducing peak velocity magnitudes.

Figure 4: **Temperature Contours for $\phi = 0.01$:**

Temperature distributions follow the expected behavior of natural convection.

At low *Ra*, heat spreads primarily via conduction with steep thermal gradients near the heated obstacles. As *Ra* increases, the contours indicate improved convective mixing with broader isotherms extending toward the top wall. Under *Ha* = 30, temperature stratification becomes more prominent, reflecting the suppressed convective motion.

Figure 5: **Velocity Contours for $\phi = 0.02$:**

With a higher volume fraction (ϕ = 0.02), the nanofluid exhibits slightly reduced flow velocities due to increased viscosity. Nevertheless, enhanced thermal conductivity promotes stronger buoyancy effects. The vortex size and strength still grow with *Ra*, though the flow remains more diffusive under magnetic damping (*Ha* = 30), confirming a subdued convection pattern.

Figure 6: **Temperature Contours for $\phi = 0.02$:**

Compared to $\phi = 0.01$, the temperature gradients near the heat sources are more evenly distributed, indicating improved heat diffusion. The top wall receives more uniform thermal flux due to the higher thermal conductivity of the nanofluid. With *Ha* = 30, thermal lines condense near the heated blocks, showing reduced vertical transport.

Figure 7: **Velocity Contours for $\phi = 0.03$:**

At ϕ = 0.03, viscous resistance increases further, slightly weakening the flow structures even at high *Ra*. The suppression due to *Ha* = 30 is particularly visible, where the streamline cores flatten and secondary vortices diminish. Still, the enhanced thermal properties at this concentration partially compensate for velocity loss, maintaining flow symmetry and structure.

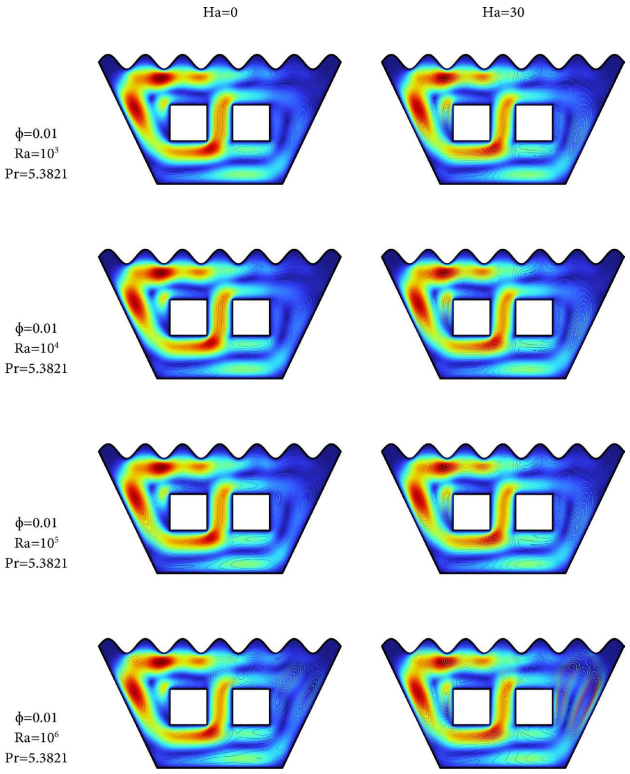

Figure 3. Velocity contour for nanoparticle volume fraction $\phi = 0.01$.

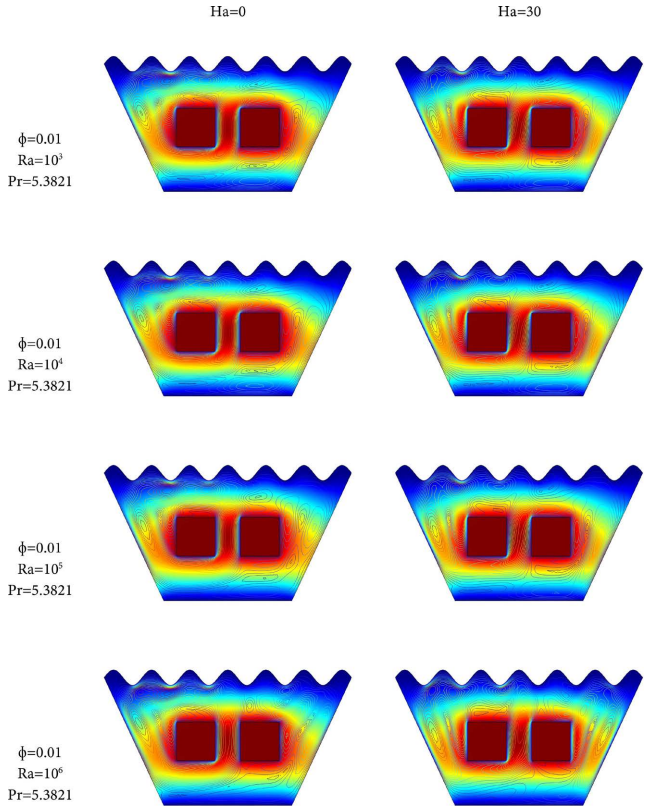

Figure 4. Temperature contour for nanoparticle volume fraction $\phi = 0.01$.

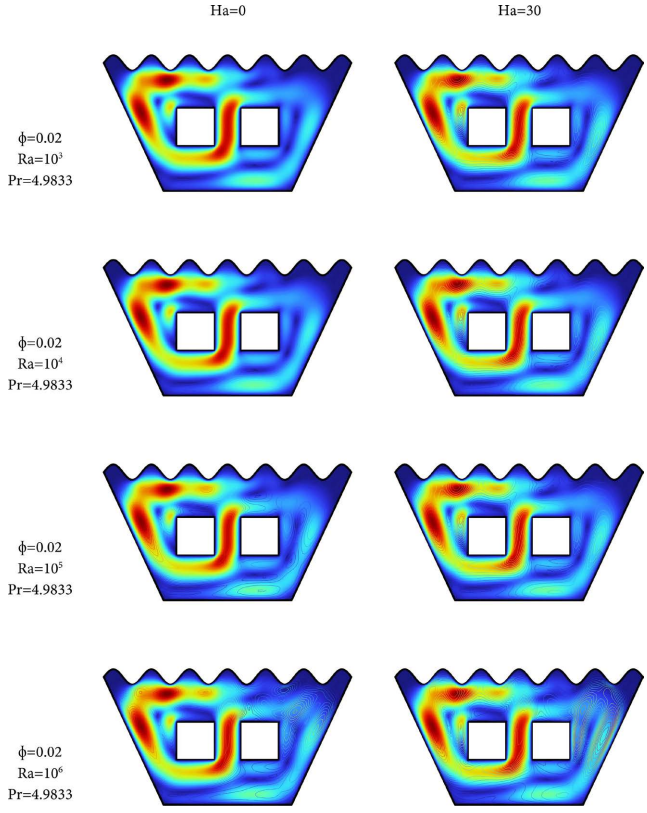

Figure 5. Velocity contour for nanoparticle volume fraction $\phi = 0.02$.

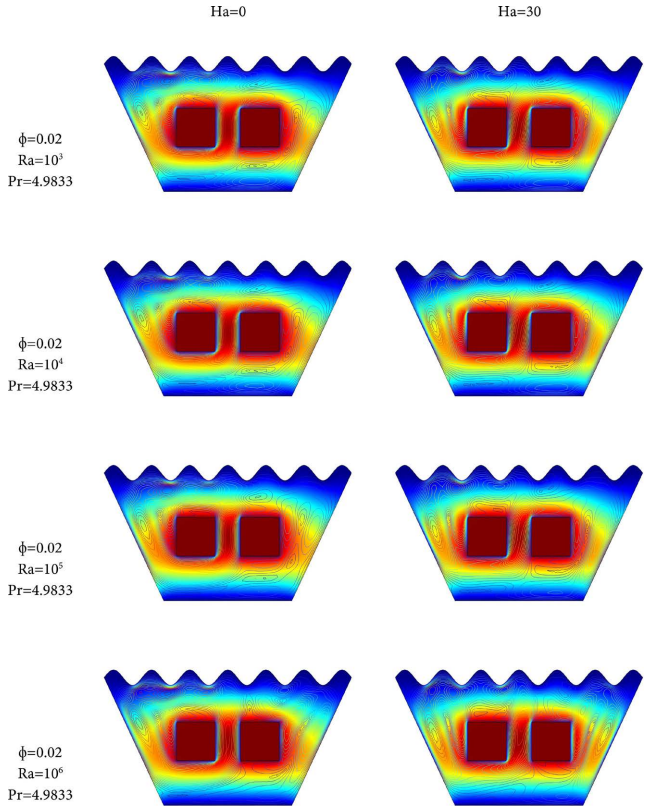

Figure 6. Temperature contour for nanoparticle volume fraction $\phi = 0.02$.

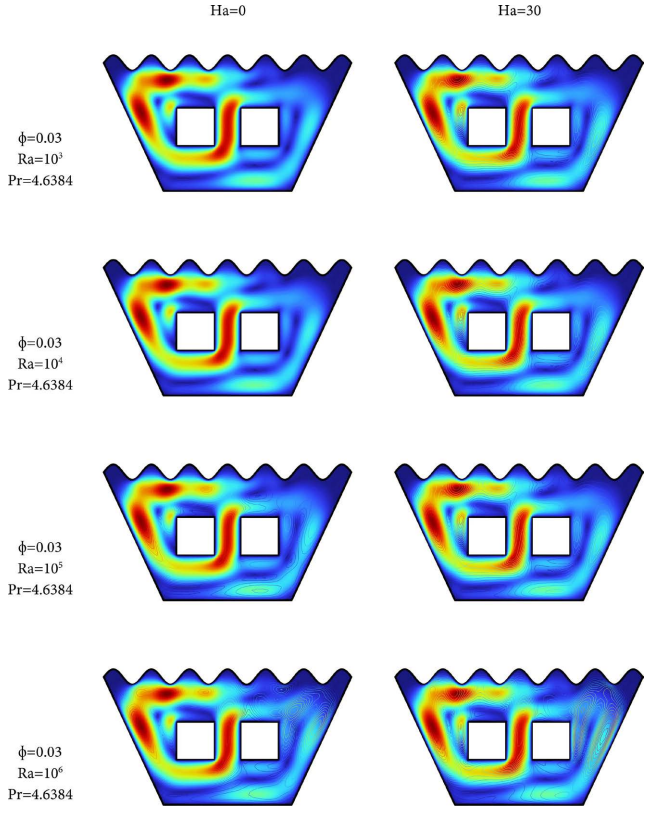

Figure 7. Velocity contour for nanoparticle volume fraction $\phi = 0.03$.

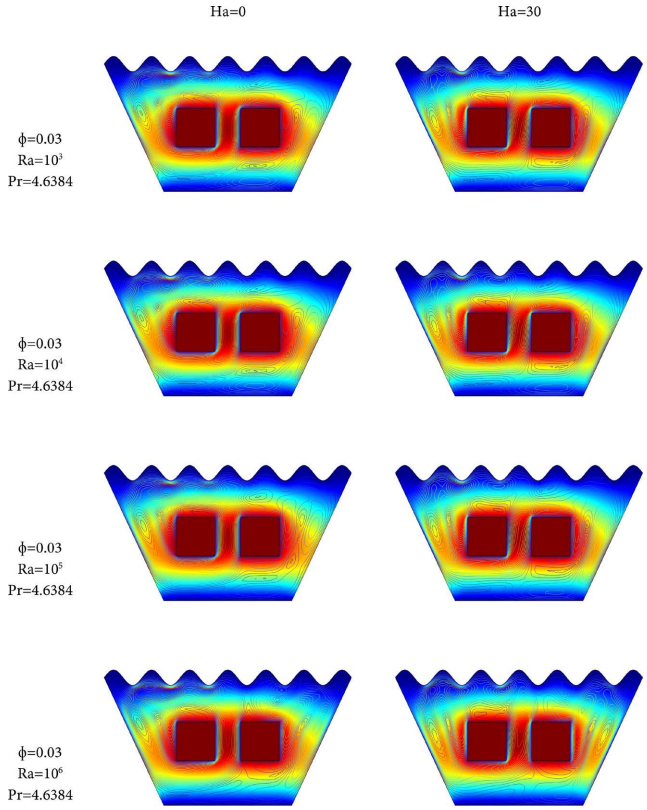

Figure 8. Temperature contour for nanoparticle volume fraction $\phi = 0.03$.

Figure 7: Velocity Contours for $\phi = 0.03$:

At $\phi = 0.03$, viscous resistance increases further, slightly weakening the flow structures even at high *Ra*. The suppression due to $Ha = 30$ is particularly visible, where the streamline cores flatten and secondary vortices diminish. Still, the enhanced thermal properties at this concentration partially compensate for velocity loss, maintaining flow symmetry and structure.

Figure 8: Temperature Contours for $\phi = 0.03$:

The temperature contours are the most uniform across all *Ra* levels at $\phi = 0.03$. Enhanced thermal conductivity leads to rapid heat dispersion from the copper blocks. However, increased thermal inertia results in flatter isotherms at higher *Ra*, particularly when $Ha = 0$. At $Ha = 30$, the thermal layer becomes sharply defined around the heated zones, reflecting the shift from convective to conductive dominance.

The results reveal that increasing the Rayleigh number (*Ra*) significantly amplifies buoyancy-driven flow, thereby intensifying convective heat transfer. This is evidenced by the development of larger and more vigorous vortical structures within the enclosure. In contrast, the application of a magnetic field ($Ha = 30$) introduces a Lorentz force that dampens fluid motion, resulting in reduced circulation intensity and more stratified temperature fields indicative of conduction-dominated heat transfer.

Furthermore, the incorporation of copper nanoparticles at higher volume frac-

tions (ϕ = 0.02 and ϕ = 0.03) leads to enhanced thermal conductivity of the nanofluid. This improvement facilitates more uniform temperature distributions and greater overall heat transfer performance. However, the increased viscosity associated with higher nanoparticle concentrations slightly diminishes flow strength, thereby indicating a trade-off between thermal enhancement and hydrodynamic resistance.

Tables 4-9 summarize the effects of Rayleigh number (Ra), nanoparticle volume fraction (ϕ), and Hartmann number (Ha) on entropy generation (S_t), thermal performance criterion (TPC), and average nanofluid temperature (T_{avf}). As Ra increases from 10^3 to 10^6, a consistent trend across all cases shows a significant rise in St, reflecting enhanced irreversibility due to stronger convection. Simultaneously, TPC decreases, indicating that while heat transfer improves, it becomes thermodynamically less efficient. T_{avf} decreases with higher Ra, demonstrating more effective convective cooling.

Table 4. For ϕ = 0.01, Pr = 5.3821 and Ha = 0.

Ra (Rayleigh Number)	S_t (Overall Entropy Generation)	TPC (Thermal Performance Criterion)	T_{avf} (Average Temperature of Nanofluid)
10^3	1.39E+08	6.89E+06	0.064655
10^4	6.50E+08	3.22E+06	0.065074
10^5	3.95E+09	1.96E+06	0.060315
10^6	2.18E+10	1.08E+06	0.042218

Table 5. For ϕ = 0.01, Pr = 5.3821 and Ha = 30.

Ra (Rayleigh Number)	S_t (Overall Entropy Generation)	TPC (Thermal Performance Criterion)	T_{avf} (Average Temperature of Nanofluid)
10^3	1.39E+08	6.89E+06	0.06467
10^4	6.49E+08	3.22E+06	0.065245
10^5	3.92E+09	1.94E+06	0.0639
10^6	2.20E+10	1.09E+06	0.047111

Table 6. For ϕ = 0.02, Pr = 4.9833 and Ha = 0.

Ra (Rayleigh Number)	S_t (Overall Entropy Generation)	TPC (Thermal Performance Criterion)	T_{avf} (Average Temperature of Nanofluid)
10^3	1.40E+08	6.95E+06	0.06276
10^4	6.56E+08	3.25E+06	0.063206
10^5	3.96E+09	1.96E+06	0.05903
10^6	2.21E+10	1.10E+06	0.041478

Table 7. For $\phi = 0.02$, $Pr = 4.9833$ and $Ha = 30$.

Ra (Rayleigh Number)	S_t (Overall Entropy Generation)	TPC (Thermal Performance Criterion)	T_{avf} (Average Temperature of Nanofluid)
10^3	1.40E+08	6.95E+06	0.062773
10^4	6.55E+08	3.25E+06	0.063358
10^5	3.93E+09	1.95E+06	0.062201
10^6	2.23E+10	1.11E+06	0.046447

Table 8. For $\phi = 0.03$, $Pr = 4.6384$ and $Ha = 0$.

Ra (Rayleigh Number)	S_t (Overall Entropy Generation)	TPC (Thermal Performance Criterion)	T_{avf} (Average Temperature of Nanofluid)
10^3	1.42E+08	7.01E+06	0.060936
10^4	6.62E+08	3.28E+06	0.061407
10^5	3.98E+09	1.97E+06	0.057745
10^6	2.25E+10	1.11E+06	0.040646

Table 9. For $\phi = 0.03$, $Pr = 4.6384$ and $Ha = 30$.

Ra (Rayleigh Number)	S_t (Overall Entropy Generation)	TPC (Thermal Performance Criterion)	T_{avf} (Average Temperature of Nanofluid)
10^3	1.42E+08	7.01E+06	0.060948
10^4	6.61E+08	3.28E+06	0.061541
10^5	3.95E+09	1.96E+06	0.060545
10^6	2.26E+10	1.12E+06	0.045806

Comparing $Ha = 0$ (Table 4, Table 6, Table 8) with $Ha = 30$ (Table 5, Table 7, Table 9), the magnetic field introduces a damping effect, slightly raising T_{avf} and S_t due to suppressed convective motion. The influence of Ha becomes more pronounced at higher Ra, where the Lorentz force counteracts buoyancy-driven flow, leading to reduced flow intensity and modified temperature profiles.

Additionally, increasing ϕ from 0.01 to 0.03 enhances thermal conductivity, resulting in lower T_{avf} and marginal increases in St due to viscous effects. TPC values are highest at low Ra and drop with increasing Ra across all ϕ levels. These observations highlight the interplay between buoyancy, magnetic suppression, and nanoparticle concentration in determining heat transfer effectiveness and entropy generation within the cavity.

Entropy generation (S_t) in this study stems from heat transfer, fluid friction, and magnetic field effects. As the Rayleigh number (Ra) increases, buoyancy-driven flow becomes stronger, resulting in greater velocity and temperature gradients that elevate entropy generation. Introducing a magnetic field ($Ha = 30$) re-

duces flow motion, thereby slightly suppressing entropy generation by limiting shear and viscous dissipation.

The Thermal Performance Criterion (TPC), defined as the ratio of total entropy generation to the average Nusselt number, decreases with increasing Ra, signifying a diminishing thermal efficiency despite higher heat transfer. This highlights the trade-off between enhancing thermal transport and managing entropy production. Tables 4-9 show this trend consistently across all tested nanoparticle volume fractions (ϕ = 0.01 - 0.03), with higher *Ra* values yielding greater St but lower TPC. Magnetic field application improves performance slightly by moderating entropy growth, and increasing ϕ marginally raises St due to increased viscosity and conductivity.

To minimize entropy generation while maximizing heat transfer, optimization strategies may include selecting moderate *Ra* values, applying appropriate magnetic field strengths, and fine-tuning nanoparticle volume fractions. These findings are particularly valuable for the thermal design of real-world systems, such as electronic cooling or energy storage devices, where both effective heat removal and thermodynamic efficiency must be carefully balanced.

5. Conclusions

This study presented a comprehensive numerical investigation of magnetohydrodynamic (MHD) free convection heat transfer in a nanofluid-filled trapezoidal cavity featuring embedded square heat sources and a wavy top wall. The enclosure was subjected to various Rayleigh (*Ra*) and Hartmann (*Ha*) numbers to analyze the thermal and flow characteristics of Cu-H_2O nanofluids at different nanoparticle volume fractions (ϕ = 0.01, 0.02, 0.03). The Boussinesq approximation was applied to model buoyancy effects, and entropy generation, thermal performance criterion (TPC), and average fluid temperature were evaluated to assess system performance.

Key Findings:

Increasing the Rayleigh number significantly enhanced convective flow intensity and heat transfer, indicated by stronger vortices and elevated entropy generation rates.

Application of a transverse magnetic field (Ha = 30) resulted in damping of convective motion due to Lorentz forces, which reduced entropy generation and flow circulation but slightly raised temperature stratification.

Enhanced thermal performance and more uniform temperature fields were observed with higher nanoparticle volume fractions, although flow strength diminished due to elevated viscosity.

The Thermal Performance Criterion (TPC) decreased with Ra, indicating stronger convective heat transport, while T_{avf} (average nanofluid temperature) dropped notably at higher *Ra* due to improved heat dissipation.

Among all cases, ϕ = 0.03 and $Ra = 10^6$ showed the best compromise between heat transfer enhancement and moderate entropy generation.

Future Work:

To extend the current research, the following directions are suggested:

Incorporating phase change materials (PCMs) and hybrid nanofluids to further improve thermal regulation.

Extending the geometry to three dimensions and introducing time-dependent boundary conditions for dynamic studies.

Experimentally validating the simulation data to establish model fidelity and extend applicability to real-world thermal systems.

Studying different obstacle shapes (circular, elliptical, star-shaped) and arrangements to assess their influence on entropy generation and heat transfer.

Integrating artificial intelligence (AI)-based surrogate modeling or optimization frameworks for real-time thermal system design and control.

Overall, this study establishes a foundational understanding of the interplay between magnetic field strength, buoyancy-driven convection, and nanofluid properties in a geometrically complex enclosure. The results highlight that optimal thermal performance can be achieved by appropriately tuning the Rayleigh number, nanoparticle concentration, and magnetic influence. These findings offer valuable insights for thermal engineers and researchers aiming to design energy-efficient systems involving nanofluids. In particular, the identified optimal configuration $\phi = 0.03$ and $Ra = 10^6$ under moderate magnetic influence can be directly applied to enhance thermal management in high-density electronic cooling systems, where rapid heat dissipation with minimal entropy generation is critical. Furthermore, these parameter settings can guide the development of more efficient thermal energy storage units by optimizing heat transfer while minimizing thermodynamic losses.

Acknowledgements

We gratefully acknowledge the **Department of Mathematics, DUET, Gazipur, Bangladesh** for their unwavering support, valuable guidance, and provision of essential facilities throughout the course of this research.

Conflicts of Interest

The authors declare no conflicts of interest regarding the publication of this paper.

References

[1] Nadeem, S., Arif, M., Ullah, I. and Alzabut, J. (2025) MHD Natural Convection of Nanofluid Flow Using a Corrugated Permeable Medium within Corrugated Circular Cavity. *Journal of Thermal Analysis and Calorimetry*, **150**, 5697-5724. https://doi.org/10.1007/s10973-025-14032-y

[2] Hameed, R.H., Hussein, R.A., Al-Salami, Q.H., Alomari, M.A., Hassan, A.M., Alyousuf, F.Q.A., *et al.* (2025) Free Convection Investigation for a Casson-Based Cu-H_2O Nanofluid in Semi Parabolic Enclosure with Corrugated Cylinder. *Heliyon*, **11**, e40960. https://doi.org/10.1016/j.heliyon.2024.e40960

[3] Mahmuda, S. and Ali, M.M. (2025) MHD Free Convection Flow of Nanofluids Inside

a Flush Mounted Heated Square Cavity Containing a Heat Conducting Triangular Cylinder. *International Journal of Applied and Computational Mathematics*, **11**, Article No. 34. https://doi.org/10.1007/s40819-025-01839-4

[4] Habiba, U., Hudha, M.N., Neogi, B., Islam, S. and Rahman, M.M. (2025) Numerical Exploration on N-Decane Nanofluid Based MHD Mixed Convection in a Lid Driven Cavity: Impact of Magnetic Field and Thermal Radiation. *International Journal of Thermofluids*, **27**, Article ID: 101209. https://doi.org/10.1016/j.ijft.2025.101209

[5] Ziaur, R.M., Azad, A.K. and Rahman, M.M. (2024) Sensitivity Study on Convective Heat Transfer in a Driven Cavity with Star-Shaped Obstacle and Hybrid Nanofluid Using Response Surface Methodology. *Heliyon*, **10**, e37440. https://doi.org/10.1016/j.heliyon.2024.e37440

[6] Qasem, N.A.A., Abderrahmane, A., Khetib, Y., Rawa, M., Abdulkadhim, A., Eldin, S.M., *et al.* (2023) Mixed Convection within Trapezoidal-Wavy Enclosure Filled with Nano-Encapsulated Phase Change Material: Effect of Magnetohydrodynamics and Wall Waviness. *Case Studies in Thermal Engineering*, **42**, Article ID: 102726. https://doi.org/10.1016/j.csite.2023.102726

[7] Alipour, N., Jafari, B. and Hosseinzadeh, K. (2023) Optimization of Wavy Trapezoidal Porous Cavity Containing Mixture Hybrid Nanofluid (Water/Ethylene Glycol Go-Al_2O_3) by Response Surface Method. *Scientific Reports*, **13**, Article No. 1635. https://doi.org/10.1038/s41598-023-28916-2

[8] Maneengam, A., Bouzennada, T., Abderrahmane, A., Ghachem, K., Kolsi, L., Younis, O., *et al.* (2022) Numerical Study of 3D MHD Mixed Convection and Entropy Generation in Trapezoidal Porous Enclosure Filled with a Hybrid Nanofluid: Effect of Zigzag Wall and Spinning Inner Cylinder. *Nanomaterials*, **12**, Article 1974. https://doi.org/10.3390/nano12121974

[9] Hirpho, M. (2021) Mixed Convection of Casson Fluid in a Differentially Heated Bottom Wavy Wall. *Heliyon*, **7**, e07361. https://doi.org/10.1016/j.heliyon.2021.e07361

[10] Ahmad, H., Mahmood, R., Hafeez, M.B., Hussain Majeed, A., Askar, S. and Shahzad, H. (2022) Thermal Visualization of Ostwald-De Waele Liquid in Wavy Trapezoidal Cavity: Effect of Undulation and Amplitude. *Case Studies in Thermal Engineering*, **29**, Article ID: 101698. https://doi.org/10.1016/j.csite.2021.101698

[11] Olayemi, O.A., Isiaka, M., Al-Farhany, K., Alomari, M.A., Ismael, M.A. and Oyedepo, S.O. (2022) Numerical Analysis of Natural Convection in a Concentric Trapezoidal Enclosure Filled with a Porous Medium. *International Journal of Engineering Research in Africa*, **61**, 129-150. https://doi.org/10.4028/p-jza9vq

[12] Uddin, M.J. and Rasel, S.K. (2019) Numerical Analysis of Natural Convective Heat Transport of Copper Oxide-Water Nanofluid Flow Inside a Quadrilateral Vessel. *Heliyon*, **5**, e01757. https://doi.org/10.1016/j.heliyon.2019.e01757

[13] Sompong, P. and Witayangkurn, S. (2013) Natural Convection in a Trapezoidal Enclosure with Wavy Top Surface. *Journal of Applied Mathematics*, **2013**, Article ID: 840632. https://doi.org/10.1155/2013/840632

[14] Mondal, P. and Mahapatra, T.R. (2020) Minimization of Entropy Generation Due to MHD Double Diffusive Mixed Convection in a Lid Driven Trapezoidal Cavity with Various Aspect Ratios. *Nonlinear Analysis: Modelling and Control*, **25**, 545-563. https://doi.org/10.15388/namc.2020.25.16774

[15] Hossain, M.S., Alim, M.A. and Andallah, L.S. (2020) Finite Element Analysis of Magnetohydrodynamic Mixed Convection in a Lid-Driven Trapezoidal Enclosure Having Heated Triangular Block. *American Journal of Computational Mathematics*, **10**, 441-

459. https://doi.org/10.4236/ajcm.2020.103025

[16] Abderrahmane, A., Younis, O., Al-Khaleel, M., Laidoudi, H., Akkurt, N., Guedri, K., *et al.* (2022) 2D MHD Mixed Convection in a Zigzag Trapezoidal Thermal Energy Storage System Using NEPCM. *Nanomaterials*, **12**, Article 3270. https://doi.org/10.3390/nano12193270

[17] Bilal, S., Shah, I.A., Ghachem, K., Aydi, A. and Kolsi, L. (2023) Heat Transfer Enhancement of MHD Natural Convection in a Star-Shaped Enclosure, Using Heated Baffle and MWCNT-Water Nanofluid. *Mathematics*, **11**, Article 1849. https://doi.org/10.3390/math11081849

[18] Ibrahim, W. and Hirpho, M. (2021) Finite Element Analysis of Mixed Convection Flow in a Trapezoidal Cavity with Non-Uniform Temperature. *Heliyon*, **7**, e05933. https://doi.org/10.1016/j.heliyon.2021.e05933

[19] Suresh Reddy, E. and Panda, S. (2022) Heat Transfer of MHD Natural Convection Casson Nanofluid Flows in a Wavy Trapezoidal Enclosure. *The European Physical Journal Special Topics*, **231**, 2733-2747. https://doi.org/10.1140/epjs/s11734-022-00609-3

[20] Hirpho, M. and Ibrahim, W. (2022) Mixed Convection Heat Transfer of a Hybrid Nanofluid in a Trapezoidal Prism with an Adiabatic Circular Cylinder. *Mathematical Problems in Engineering*, **2022**, Article ID: 8170224. https://doi.org/10.1155/2022/8170224

[21] Hussein, A.K., Hamzah, H.K., Ali, F.H. and Kolsi, L. (2019) Mixed Convection in a Trapezoidal Enclosure Filled with Two Layers of Nanofluid and Porous Media with a Rotating Circular Cylinder and a Sinusoidal Bottom Wall. *Journal of Thermal Analysis and Calorimetry*, **141**, 2061-2079. https://doi.org/10.1007/s10973-019-08963-6

[22] Selimefendigil, F. (2017) Natural Convection in a Trapezoidal Cavity with an Inner Conductive Object of Different Shapes and Filled with Nanofluids of Different Nanoparticle Shapes. *Iranian Journal of Science and Technology, Transactions of Mechanical Engineering*, **42**, 169-184. https://doi.org/10.1007/s40997-017-0083-3

[23] Mahmood, R., Khan, Y., Rahman, N., Majeed, A.H., Alameer, A. and Faraz, N. (2022) Numerical Computations of Entropy Generation and MHD Ferrofluid Filled in a Closed Wavy Configuration: Finite Element Based Study. *Frontiers in Physics*, **10**, Article 916394. https://doi.org/10.3389/fphy.2022.916394

[24] Job, V.M., Gunakala, S.R. and Chamkha, A.J. (2022) Numerical Investigation of Unsteady MHD Mixed Convective Flow of Hybrid Nanofluid in a Corrugated Trapezoidal Cavity with Internal Rotating Heat-Generating Solid Cylinder. *The European Physical Journal Special Topics*, **231**, 2661-2668. https://doi.org/10.1140/epjs/s11734-022-00604-8

[25] Alshuraiaan, B. and Pop, I. (2021) Numerical Simulation of Mixed Convection in a Lid-Driven Trapezoidal Cavity with Flexible Bottom Wall and Filled with a Hybrid Nanofluid. *The European Physical Journal Plus*, **136**, Article No. 580. https://doi.org/10.1140/epjp/s13360-021-01349-4

[26] Alomari, M.A., Al-Farhany, K., Hashem, A.L., Al-Dawody, M.F., Redouane, F. and Olayemi, O.A. (2021) Numerical Study of MHD Natural Convection in Trapezoidal Enclosure Filled with (50%MgO-50%ag/Water) Hybrid Nanofluid: Heated Sinusoidal from Below. *International Journal of Heat and Technology*, **39**, 1271-1279. https://doi.org/10.18280/ijht.390425

[27] Dogonchi, A.S., Sadeghi, M.S., Ghodrat, M., Chamkha, A.J., Elmasry, Y. and Alsulami, R. (2021) Natural Convection and Entropy Generation of a Nanoliquid in a

Crown Wavy Cavity: Effect of Thermo-Physical Parameters and Cavity Shape. *Case Studies in Thermal Engineering*, **27**, Article ID: 101208. https://doi.org/10.1016/j.csite.2021.101208

[28] Alsabery, A.I., Tayebi, T., Kadhim, H.T., Ghalambaz, M., Hashim, I. and Chamkha, A.J. (2021) Impact of Two-Phase Hybrid Nanofluid Approach on Mixed Convection Inside Wavy Lid-Driven Cavity Having Localized Solid Block. *Journal of Advanced Research*, **30**, 63-74. https://doi.org/10.1016/j.jare.2020.09.008

[29] Zeb Khan, N., Bilal, S., Riaz, A. and Muhammad, T. (2024) Coupled Effects of Variable Permeability and Adiabatic Undulating Walls on Natural Convective Flow in a Trapezoidal Cavity: Finite Element Analysis. *Results in Physics*, **56**, Article ID: 107267. https://doi.org/10.1016/j.rinp.2023.107267

[30] Mohammed, A.A., Thaer, M. and Yahya, D.Q. (2022) Mixed Convection Heat Transfer of Al_2O_3-H_2O Nanofluid in a Trapezoidal Lid-Driven Cavity at Different Angles of Inclination. *Texas Journal of Engineering and Technology*, **11**, 20-30.

[31] Uddin, M.N., Alim, M.A. and Bhuiyan, A.H. (2016) Effects of Circular Cylindrical Block on Heat Flow for MHD Free Convection in a Non-Uniformly Heated Trapezoidal Enclosure. *International Journal of Engineering & Applied Sciences*, **8**, 40-48. https://doi.org/10.24107/ijeas.255034

[32] Alnajem, M.H.S., Alsabery, A.I. and Hashim, I. (2019) Entropy Generation and Natural Convection in a Wavy-Wall Cavity Filled with a Nanofluid and Containing an Inner Solid Cylinder. *IOP Conference Series*: *Materials Science and Engineering*, **518**, Article ID: 032044. https://doi.org/10.1088/1757-899x/518/3/032044

[33] Mejbel, A., Abdulkadhim, A., Hamzah, R., Hamzah, H. and Ali, F. (2020) Natural Convection Heat Transfer for Adiabatic Circular Cylinder Inside Trapezoidal Enclosure Filled with Nanofluid Superposed Porous-Nanofluid Layer. *FME Transactions*, **48**, 82-89. https://doi.org/10.5937/fmet2001082m

[34] Ali, M.Y., Alim, M.A. and Karim, M.M. (2023) Mixed Convective Heat Transfer Analysis by Heatlines on a Lid-Driven Cavity Having Heated Wavy Wall Containing Tilted Square Obstacle. *Mathematical Problems in Engineering*, **2023**, Article ID: 1374926. https://doi.org/10.1155/2023/1374926

[35] Alesbe, I., Ibrahim, S.H. and Aljabair, S. (2021) Mixed Convection Heat Transfer in Multi-Lid-Driven Trapezoidal Annulus Filled with Hybrid Nanofluid. *Journal of Physics*: *Conference Series*, **1973**, Article ID: 012065. https://doi.org/10.1088/1742-6596/1973/1/012065

[36] Akter, A. and Parvin, S. (2018) Analysis of Natural Convection Flow in a Trapezoidal Cavity Containing a Rectangular Heated Body in Presence of External Oriented Magnetic Field. *Journal of Scientific Research*, **10**, 11-23. https://doi.org/10.3329/jsr.v10i1.33848

[37] Ishak, M.S., Alsabery, A.I., Hashim, I. and Chamkha, A.J. (2021) Entropy Production and Mixed Convection within Trapezoidal Cavity Having Nanofluids and Localised Solid Cylinder. *Scientific Reports*, **11**, Article No. 14700. https://doi.org/10.1038/s41598-021-94238-w

[38] Chowdhury, K. and Alim, M.A. (2023) Mixed Convection in a Double Lid-Driven Wavy Shaped Cavity Filled with Nanofluid Subject to Magnetic Field and Internal Heat Source. *Journal of Applied Mathematics*, **2023**, Article ID: 7117186. https://doi.org/10.1155/2023/7117186

[39] Alsabery, A.I., Vaezi, M., Tayebi, T., Hashim, I., Ghalambaz, M. and Chamkha, A.J. (2022) Nanofluid Mixed Convection Inside Wavy Cavity with Heat Source: A Non-Homogeneous Study. *Case Studies in Thermal Engineering*, **34**, Article ID: 102049.

https://doi.org/10.1016/j.csite.2022.102049

[40] Alsabery, A.I., Ghalambaz, M., Armaghani, T., Chamkha, A., Hashim, I. and Saffari Pour, M. (2020) Role of Rotating Cylinder toward Mixed Convection Inside a Wavy Heated Cavity via Two-Phase Nanofluid Concept. *Nanomaterials*, **10**, Article 1138. https://doi.org/10.3390/nano10061138

[41] Ashorynejad, H.R. and Shahriari, A. (2018) MHD Natural Convection of Hybrid Nanofluid in an Open Wavy Cavity. *Results in Physics*, **9**, 440-455. https://doi.org/10.1016/j.rinp.2018.02.045

[42] Boulahia, Z., Wakif, A., Chamkha, A.J., Amanulla, C.H. and Sehaqui, R. (2018) Effects of Wavy Wall Amplitudes on Mixed Convection Heat Transfer in a Ventilated Wavy Cavity Filled by Copper-Water Nanofluid Containing a Central Circular Cold Body. *Journal of Nanofluids*, **8**, 1170-1178. https://doi.org/10.1166/jon.2019.1654

[43] Rabbi, K.M., Saha, S., Mojumder, S., Rahman, M.M., Saidur, R. and Ibrahim, T.A. (2016) Numerical Investigation of Pure Mixed Convection in a Ferrofluid-Filled Lid-Driven Cavity for Different Heater Configurations. *Alexandria Engineering Journal*, **55**, 127-139. https://doi.org/10.1016/j.aej.2015.12.021

[44] Toghraie, D. (2020) Numerical Simulation on MHD Mixed Convection of Cu-Water Nanofluid in a Trapezoidal Lid-Driven Cavity. *International Journal of Applied Electromagnetics and Mechanics*, **62**, 683-710. https://doi.org/10.3233/jae-190123

[45] Mahmud, M.J., Rais, A.I., Hossain, M.R. and Saha, S. (2022) Conjugate Mixed Convection Heat Transfer with Internal Heat Generation in a Lid-Driven Enclosure with Spinning Solid Cylinder. *Heliyon*, **8**, e11968. https://doi.org/10.1016/j.heliyon.2022.e11968